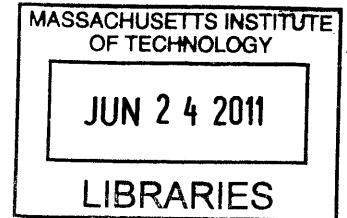


# Theory of Piezoelectric Materials and Their Applications in Civil Engineering

By

Antoine Ledoux  
French Engineer Degree  
Ecole Centrale Paris



Submitted to the Department of Civil and Environmental Engineering in partial fulfillment of the requirements for the degree of

MASTER OF ENGINEERING IN CIVIL AND ENVIRONMENTAL ENGINEERING  
AT THE  
MASSACHUSETTS INSTITUTE OF TECHNOLOGY

**ARCHIVES**

JUNE 2011

©2011 Antoine Ledoux. All rights reserved.

The author hereby grants to MIT permission to reproduce  
and to distribute publicly paper and electronic copies  
of this thesis document in whole or in part  
in any medium now known or hereafter created.

Signature of author: \_\_\_\_\_  
Department of Civil and Environmental Engineering  
May 13, 2011

Certified by: \_\_\_\_\_  
Jerome J. Connor  
Professor of Civil and Environmental Engineering  
Thesis Supervisor

Accepted by: \_\_\_\_\_  
Heidi M. Nepf  
Chair, Departmental Committee for Graduate Students

# **Theory of Piezoelectric Materials and Their Applications in Civil Engineering**

By  
Antoine Ledoux

Submitted to the Department of Civil and Environmental Engineering  
on May 13, 2011 in Partial Fulfillment of the requirements for the degree of  
Master of Engineering in Civil and Environmental Engineering

## **1 Abstract**

The goal of this thesis is to explore ways of harvesting energy from a building. To be more specific, the conversion of mechanical energy into electrical energy using piezoelectric materials is studied. Applications of piezoelectric materials as actuators are also explored, with particular interest in the question: what is the maximum moment that an actuator, whose energy comes from piezoelectricity, can develop when attached to a beam. As a piezoelectric material cannot generate much energy, and often requires amplification, the goal is to optimize the circuit linked to the piezoelectric material to obtain as much power as possible.

Thesis Supervisor: Jerome Connor  
Title: Professor of Civil and Environmental Engineering

# Contents

<b>1</b>	<b>Abstract</b>	
<b>2</b>	<b>Acknowledgements</b>	<b>6</b>
<b>3</b>	<b>Introduction to Piezoelectric Materials and their Properties</b>	<b>7</b>
3.1	Overall Concept . . . . .	7
3.2	History . . . . .	7
3.3	How it Works? . . . . .	8
3.4	How Are They Made? . . . . .	9
3.5	Examples of Piezoelectric Materials . . . . .	11
<b>4</b>	<b>Device Concept</b>	<b>13</b>
<b>5</b>	<b>Theory</b>	<b>15</b>
5.1	Mathematical Description . . . . .	15
5.2	Development of Equations . . . . .	17
<b>6</b>	<b>Application in Civil Engineering</b>	<b>20</b>
6.1	Tuned-Mass Damper . . . . .	20
6.2	Actuators on Multi-Span Beams . . . . .	31
<b>7</b>	<b>Conclusion</b>	<b>38</b>
<b>A</b>	<b>Stiffness Calculations</b>	<b>40</b>
<b>B</b>	<b>Mathematica Code</b>	<b>41</b>

## List of Figures

1	Crystalline structure of a ceramic piezoelectric material b) with and a) without a dipole $\vec{P}$ . . . . .	9
2	Method to pole a piezoelectric material . . . . .	10
3	Hysteretic curve of polarization . . . . .	11
4	Schematic of Piezoelectric Power Generator . . . . .	14
5	Model of the Tuned Mass Damper . . . . .	21
6	Curve of $H_1$ as a function of $\rho$ for $\xi_d = 0, 0.05$ and $0.1$ in purple, pink and maroon respectively . . . . .	24
7	Curve of $H_1$ as a function of $\rho$ and $\xi_d$ . . . . .	24
8	Sketch of the device that is studied . . . . .	25
9	Sketch of the modelisation of the device that is studied . . . . .	27
10	Mathematica file showing a plot of $H_p$ as a function of $\rho$ for $\xi_d=0, 0.2$ and $0.4$ in purple, pink and maroon respectively . . . . .	29
11	Mathematica file showing a 3D plot of $H_p$ as a function of $\xi_d$ and $\rho$ . . . . .	29
12	Generic Diagram Representation of a Control Algorithm . . . . .	32
13	Mathematica file showing the bending moment in a beam with a unit point load running along a beam of length $L=10$ (it is an animated file, a click on play would animate the feature) . . . . .	33
14	Mathematica file showing the distribution of the bending moments across the beam with the unit point load positioned at 15 ft from the edge of the beam. . . . .	34
15	Mathematica file showing the distribution of the bending moments across the beam with the unit point load positioned at 49.25 ft from the edge of the beam. . . . .	35
16	Mathematica file showing amplitude of the actuators when the unit point load is situated at $a=5.15$ ft . . . . .	36
17	Mathematica file showing the resulting moments after the actuators have been activated . . . . .	37

18 Sketch of the curve of the cantilever for stiffness calculation . . . . . 40

## 2 Acknowledgements

There are many people who I would like to thank for their support while I was writing this thesis.

First and foremost, I would like to thank Professor Connor for his valuable advice and support. Professor Connor has always been there for me when I needed him, helping me when I was stuck, reassuring me when I was preoccupied and guiding when I was lost.

Secondly, I would like to thank Simon Laflamme whose advice, open-mindedness and sense of humor has always been a good way to motivate me and make writing this thesis a pleasure.

Also, I would like to thank all my classmates who supported me while we were working on this thesis for long hours in the M.Eng room. I would like to thank Karen for her sense of humor, she is too funny, Andrew for his sense of humor, he is very funny too, and Miryam for her emotional support.

I would also like to thank my friend Guillaume who came from Paris to spend 10 days at my place in Boston while I was working on this thesis and was always there for me to drink a beer and relax after having spent countless hours in the M.Eng room.

Finally, I would like to thank my parents who have always been there for me, and above all who made this amazing experience at MIT possible. Thank you Mom. Thank you Dad.

## **3 Introduction to Piezoelectric Materials and their Properties**

### **3.1 Overall Concept**

Nowadays, most of the research in the energy field is to develop sources of energy for future. With oil resources being over tapped and eventually bound to end, it is time to find renewable sources of energy for the future. Piezoelectric materials are being more and more studied as they turn out to be very unusual materials with very specific and interesting properties. In fact, these materials have the ability to produce electrical energy from mechanical energy, for example they can convert mechanical behavior like vibrations into electricity. Such devices are commonly referred to as energy harvesters and can be used in applications where outside power is unavailable and batteries are not a feasible option. While recent experiments have shown that these materials could be used as power generators, the amount of energy produced is still very low, hence the necessity to optimize them.

### **3.2 History**

The piezoelectric effect was discovered in 1880 by the brothers Pierre Curie and Jacques Curie. They combined what they knew about pyroelectricity and about structures of crystals to demonstrate the effect with tourmaline, quartz, topaz, cane sugar and Rochelle salt. They found out that when a mechanical stress was applied on these crystals, electricity was produced and the voltage of these electrical charges was proportional to the stress. The converse effect however was discovered later by Gabriel Lippmann in 1881 through the mathematical aspect of the theory. These behaviors were labeled the piezoelectric effect and the inverse piezoelectric effect, respectively, from the Greek word piezein, meaning to press or squeeze. The first applications were made during World War I with piezoelectric ultrasonic transducers. Nowadays, piezoelectricity is used in everyday life. For example, in the car's airbag

sensor where the material detects the change in acceleration of the car by sending an electrical signal which triggers the airbag [1].

### 3.3 How it Works?

The nature of piezoelectric materials is closely linked to the significant quantity of electric dipoles within these materials. These dipoles can either be induced by ions on crystal lattice sites with asymmetric charge surroundings (as in BaTiO<sub>3</sub> and PZTs, see section *Examples of Piezoelectric Materials* for more explanations on these materials) or by certain molecular groups with electrical properties. A dipole is a vector, often named  $\vec{P}$ , so it has a direction and a value in accordance with the electrical charges around. These dipoles tend to have the same direction when next to each other, and they altogether form regions called Weiss domains. The domains are generally randomly oriented but they can be aligned using the process of poling, which is a process by which a strong electric field is applied across the material (see next section *How Are They Made?*). However not every piezoelectric materials can be poled. The reason why piezoelectric material creates a voltage is because when a mechanical stress is applied, the crystalline structure is disturbed and it changes the direction of the polarization  $\vec{P}$  of the electric dipoles. Depending on the nature of the dipole (if it is induced by ion or molecular groups), this change in the polarization might either be caused by a re-configuration of the ions within the crystalline structure or by a re-orientation of molecular groups [2]. As a consequence, the bigger the mechanical stress, the bigger the change in polarization and the more electricity is produced. A traditional piezoelectric ceramic is a mass of perovskite ceramic crystals, each consisting of a small, tetravalent metal ion, usually titanium or zirconium (see Figure 1), in a lattice of larger, divalent metal ions, usually lead or barium, and O<sub>2</sub>-ions. Under conditions that confer tetragonal or rhombohedral symmetry on the crystals, each crystal has a dipole moment. The change in  $\vec{P}$  appears as a variation of surface charge density upon the crystal faces, i.e. as a variation of the electrical field extending between the faces. For example, a 1 cm<sup>3</sup>



cube of quartz with 2 kN (500 lbf) of correctly applied force can produce a voltage of 12500 V [3] [4].

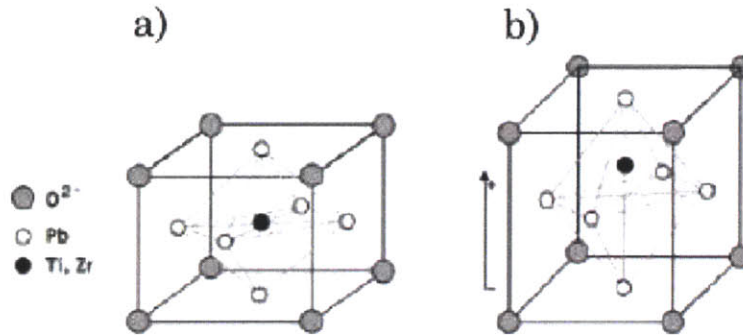


Figure 1: Crystalline structure of a ceramic piezoelectric material b) with and a) without a dipole  $\vec{P}$

### 3.4 How Are They Made?

Piezoelectric materials can be natural or man-made. The most common natural piezoelectric material is quartz (see next section for more details), but man-made piezoelectric materials are more efficient and mostly ceramics. Due to their complex crystalline structure, the process with which they are made is very precise and has to follow very specific steps. As explained in *Electroceramics: Materials, Properties and Applications* [5], to prepare a piezoelectric ceramic, "fine PZT powders of the component metal oxides are mixed in specific proportions, then heated to form a uniform powder. The piezo powder is mixed with an organic binder and is formed into structural elements having the desired shape (discs, rods, plates, etc.). The elements are fired according to a specific time and temperature program, during which the piezo powder particles sinter and the material attains a dense crystalline structure. The elements are cooled, then shaped or trimmed to specifications, and electrodes are

*applied to the appropriate surfaces."*

However, piezoelectric material exhibits an electric behavior and acts as a dipole only below a certain temperature called Curie temperature. Above the Curie point, the crystalline structure will have a simple cubic symmetry so no dipole moment (see first sketch of Figure 1). On the contrary, below the Curie point, the crystal will have a tetragonal or rhombihedral symmetry hence a dipole moment (see second sketch of Figure 1). As explained earlier in this report, adjoining dipoles form regions called Weiss domains and exhibit a larger dipole moment as every dipole in the domain has roughly the same direction, thus a net polarization. The change of direction of polarization between two neighboring domains is random, making the whole material neutral with no overall polarization (see first sketch of Figure 2).

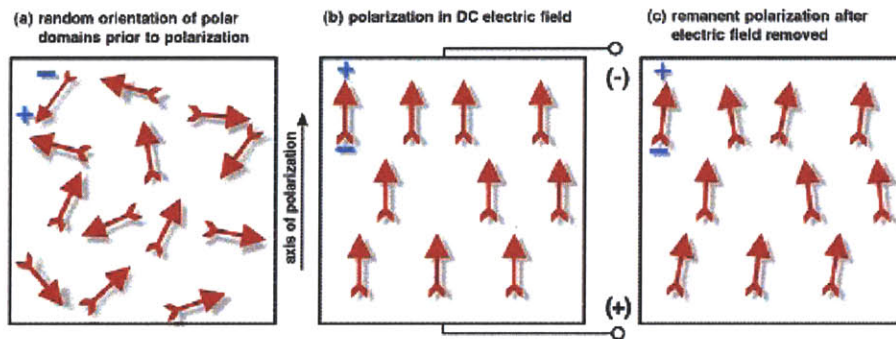


Figure 2: Method to pole a piezoelectric material

In order for the material to be polarized, it is exposed to a strong and direct current electric field whose goal is to align all dipoles in the material. Of course this transformation has to be made below the Curie point so that dipoles are present. Thanks to this polarization, the material gets its dipoles almost aligned with the electric field and now has a permanent polarization. This permanent polarization is the remanent polarization after the electric field is removed, due to a hysteretic behavior (Figure 3) and it also gets lengthen in the direction of the field (see second sketch of Figure 1), for the same hysteretic reason[6].

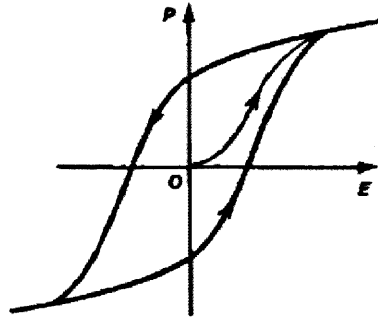


Figure 3: Hysteretic curve of polarization

### 3.5 Examples of Piezoelectric Materials

The most commonly known piezoelectric material is quartz. But piezoelectric materials are numerous, the most used are :

- Quartz ( $SiO_2$ ) : Quartz shows a strong piezoelectricity due to its crystalline structure, meaning that when a pressure is applied on a quartz crystal an electrical polarization can be observed along the pressure direction.
- Berlinite ( $AlPO_4$ )
- Gallium orthophosphate ( $GaPO_4$ ) : Gallium orthophosphate has almost the same crystalline structure as quartz, that is why it has the same characteristics. However its piezoelectric effect is almost twice as important as the one for the quartz, making it a valuable asset for mechanical application. It is not a natural element, it has to be synthesised.
- Tourmaline : crystal commonly black but can range from violet to green and pink.
- Barium Titanate ( $BaTiO_3$ ) : This element is an electrical ceramics, it is usually replaced by lead zirconate titanate ( $PZT$ ) for piezoelectricity. It is used for microphones and transducers.

- Lead Zirconate Titanate (*PZT*) : It is considered today one of the most economical piezoelectric element, hence it is used in a lot of applications.
- Zinc oxide (*ZnO*)
- Aluminum Nitride (*AlN*)
- Polyvinylidene Fluoride (*PVDF*)

## 4 Device Concept

In order to extract the electrical energy produced by the piezoelectric material, it is necessary to connect it to a circuit. For a power generator, the goal is to convert a maximum amount of mechanical energy into electrical energy, that will provide a great amount of current. Thus a resonant circuit is ideally suited to harvest a maximum amount of current from the oscillator. In fact, a resonant circuit is only composed of passive electrical components such as capacitors, inductors and resistors and does not need an outside source of energy that could disturb the extraction of energy from the oscillator. Also, such a resonant circuit is analogous to a mechanical system composed of masses and springs, which is what the oscillator is, making easier the combination with the latter [7]. The field of civil engineering finds applications with piezoelectric material and has an interest in optimizing them, this area of study is also known as Motion Based Design. The Motion Based Design methodology attempts to satisfy the design requirements of a structure such as displacements and/or accelerations while assuring appropriate strength capacity. Indeed, by optimally proportioning stiffness and damping throughout a structure and/or through the use of motion control devices, kinematic constraints of a structure subjected to a given loading can be approximately realized [8]. One of the most common method of motion control is the use of Tuned-Mass Dampers (TMD). A TMD is a system put on top of a building (usually modeled as a mass and a spring) specially designed so that it moves out of phase with the structure when it is subjected to a loading such as an earthquake, making the building more stable by significantly reducing the motion of the building.

The device that is studied in this thesis is a horizontal clamped beam submitted to oscillation with piezoelectric material at its base (where strain is the highest : so more current is produced by the material here). This material is linked to a shunting circuit (see Figure 4 below). The study of such a device might seem irrelevant and far from what happens in reality but part of the device has a different stiffness due to

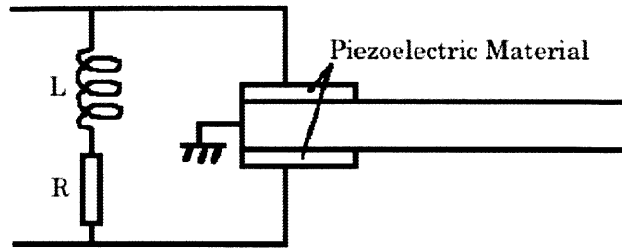


Figure 4: Schematic of Piezoelectric Power Generator

the presence of piezoelectric material and the frequency of that part of the cantilever depends on the properties of the shunting circuit, making this part of the device quite independent and the whole system similar to a main structure with a TMD attached to it (see section *Tuned – Mass Dampers* for more details on the subject).

## 5 Theory

The aim of the theory is to describe mathematically the material behavior. However, the equations governing piezoelectricity involve entities that cannot be measured experimentally, thus they need to be converted so that they make sense for experiments and common use.

### 5.1 Mathematical Description

A piezoelectric material develops an internal electric field when strained. On the contrary, a piezoelectric material experiences strain when an electrical field is applied to it. These reactions, electrical field and mechanical behavior, can be in either directions. Meaning that depending on the material, an electrical field in one direction can lead to a mechanical reaction in any direction. As a result, equations governing piezoelectricity are usually expressed with tensors. However, to avoid any complicated calculations, one can consider materials which produce an electric field in only one direction, either parallel or perpendicular to the strain that is applied to it. Equations thus become (assuming no variation in temperature and low frequencies):

$$\vec{D} = d_1 \vec{T} + \epsilon^T \vec{E}$$

$$\vec{S} = s^E \vec{T} + d_2 \vec{E}$$

$\vec{D}$  : electric displacement

$d_1$  and  $d_2$  : piezoelectric charge coefficients, respectively for the direct piezoelectric effect and the converse piezoelectric effect

$\vec{T}$  : mechanical stress

$\epsilon^T$  : permittivity at constant stress

$\vec{E}$  : electric field

$\vec{S}$  : mechanical strain

$s^E$  : mechanical compliance

These expressions show the relationship between the mechanical and the electrical behaviors of those materials. The first equation shows that part of an electrical field applied to the material is converted into mechanical stress. Likewise, the second equation shows that part of a mechanical strain applied to the material is converted into electrical field. One can note that in the absence of electric field  $\vec{E}$ , the second equation is  $\vec{S} = s^E \vec{T}$  which is Hooke's Law. Likewise, in the absence of mechanical stress the first equation is  $\vec{D} = \epsilon^T \vec{E}$ , only describing the electrical behavior of the material. Also, for most materials  $d_1$  and  $d_2$  are nearly equal, that is why they are taken to be both equal to  $d$ , hence:

$$\vec{S} = s^E(1 - k^2)\vec{T} + \frac{d}{\epsilon^T}\vec{D}$$

$$k^2 = \frac{d^2}{s^E \epsilon^T}$$

where  $k$  is known as the electromechanical coupling coefficient. It is an indicator of the effectiveness with which a piezoelectric material converts electrical energy into mechanical energy, or converts mechanical energy into electrical energy. In the case where the electric displacement is equal to zero, the formula becomes :

$$\vec{S} = s^E(1 - k^2)\vec{T}$$

The strain is still proportional to the stress, but the compliance is multiplied by the term  $(1 - k^2)$ . When  $k$  is equal to zero, the equation is simply Hooke's Law, which is logical as it means that all the energy in the material is strain energy. However one must know that this expression of  $k$  has been obtained considering that the system is not connected to a circuit. An new expression of  $k$  in the case of a system linked to a circuit is now developed.



## 5.2 Development of Equations

First, one must think in terms of currents and voltages since these entities can be measured easily on a circuit, in contrast to the electric displacement and electric field. To replace the electric displacement and the electric field in the above equations, one must realize that a constant electric displacement results in zero current hence the fact that these two entities are linked. Likewise a zero electric field results in a zero voltage. The following expressions describe mathematically these experimental results:

$$V = \int_0^x \vec{E} \cdot d\vec{x}$$
$$I = \frac{\partial}{\partial t} \int_A \vec{D} \cdot d\vec{a}$$

with :

$I$  : Current

$V$  : Voltage

$x$  : thickness of the piezoelectric material

$A$  : surface area of the piezoelectric material

$\vec{E}$  : electric field

$\vec{D}$  : electric displacement

As a consequence, the applied stress on the material will develop a voltage and a current in the circuit linked to the piezoelectric material. These expressions can be simplified and mixed with the previous original equations describing piezoelectricity assuming the electric field  $\vec{E}$  is uniform along the thickness of the material and the electric displacement  $\vec{D}$  is uniform on the material's surface, and taking Laplace transform :

$$V(s) = \vec{E}(s) \cdot \vec{x}$$

$$I(s) = s \cdot \vec{A} \cdot \vec{D}(s)$$

where  $s$  is the Laplace parameter. Still working in the Laplace domain, one can obtain :

$$I(s) = s C V(s) + s A d T(s)$$

$$S(s) = \frac{d}{x} V(s) + s^E T(s)$$

with :

$$C = \frac{A \epsilon^T}{x}$$

where  $C$  is also known as the inherent open circuit capacitance of the piezoelectric material, and then suppressing  $T(s)$  and  $V(s)$  :

$$I(s) = s C (1 - k^2) V(s) + \frac{s A \epsilon^T k^2}{d} S(s)$$

$$S(s) = \frac{k^2 s^E}{d A s} I(s) + s^E (1 - k^2) T(s)$$

In the first equation, one can notice that even if the voltage is equal to zero the current will not be equal to zero, which means that there is a source of current in the circuit. This source of current is of course the piezoelectric material, submitted to a mechanical loading. Also, on the contrary to the previous relation between stress and strain, there is a new term out of phase included in the second equation. In other words, the simple proportionality between stress and strain is lost as soon as both electrical and displacements fields are not equal to zero. Finally, when  $k$  is equal to zero, the second equation becomes Hooke's Law, which is logical.

Now putting the above equations in matrix form:

$$\begin{bmatrix} I \\ S \end{bmatrix} = \begin{bmatrix} sC & sAd \\ \frac{d}{x} & s^E \end{bmatrix} \begin{bmatrix} V \\ T \end{bmatrix}$$

The term in the upper left corner of the above matrix is an admittance, it is the admittance of the piezoelectric effect. When a circuit of impedance  $Z_{ext}$  is connected, its admittance is added to that of the piezoelectric, leading to the following equation:

$$\begin{bmatrix} I \\ S \end{bmatrix} = \begin{bmatrix} sC + \frac{1}{Z_{ext}} & sAd \\ \frac{d}{x} & s^E \end{bmatrix} \begin{bmatrix} V \\ T \end{bmatrix}$$

One can calculate the new  $k$  when a circuit is linked to the material by using the ratio of the amount of electrical energy produced to the total energy in the system. The final result is:

$$k_{gen}^2 = k^2 \frac{sCZ_{ext}}{1 + sCZ_{ext}}$$

[7]

Now replacing  $k$  by  $k_{gen}$  gives:

$$\vec{S} = s^E(1 - k_{gen}^2)\vec{T}$$

## 6 Application in Civil Engineering

### 6.1 Tuned-Mass Damper

A tuned mass damper (TMD) is composed of a mass, a spring and a damper and is supposed to reduce the dynamic response of the structure to which it is attached. The values of the mass, the spring and the damper of the TMD are calculated so that the TMD will resonate out of phase with the structure when excited by an external loading. It is basically a damping system that minimizes the displacement of the main mass with a combination of both its spring and its viscous damping. The concept of TMD was first set by Frahm in 1909 and was applied to ship hull vibrations. The theory came later with a paper by Ormondroyd and Den Hartog in 1928 but many researchers have studied the subject since then, studying the optimum TMD for single-degree-of-freedom system and extending it to multi-degree-of-freedom systems [8]. The TMD and the main structure form a two-degree-of-freedom system, if the structure is modeled as a one-degree-of-freedom system of course. Here the idea is to provide electricity by attaching piezoelectric material to the TMD, and then to optimize the system so that a maximum of energy is given to that TMD, thus producing a maximum of energy. One can see on Figure 5 the system with the TMD on top of the main structure.

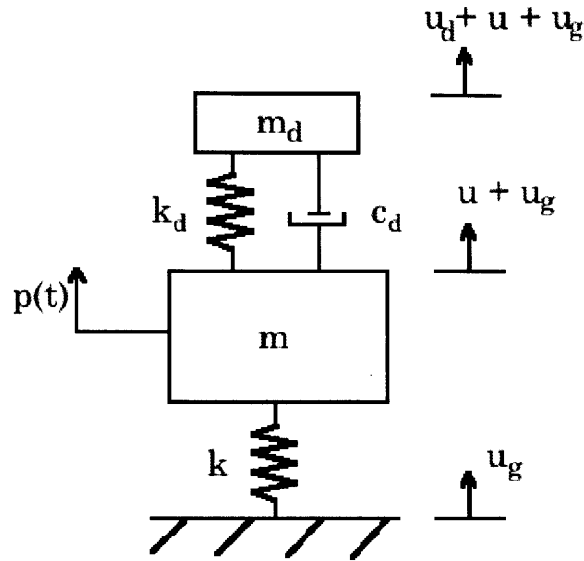


Figure 5: Model of the Tuned Mass Damper

The equations governing this system are as follows :

$$m_d \ddot{u}_d + c_d \dot{u}_d + k_d u_d + m_d \ddot{u} = -m_d \ddot{u}_g$$

$$m \ddot{u} + k u - c_d \dot{u}_d - k_d u_d = p(t) - m \ddot{u}_g$$

with:

$m_d$  : damper mass

$m$  : main mass

$k_d$  : spring constant of the damper system

$k$  : spring constant of the main system

$c_d$  : viscous damping of the damper system

$x_d$  : displacement of the damper system

$x$  : displacement of the main system

$p(t)$  : load on the main system

The presence of damping induces a phase shift between the response and the excitation. It is more convenient to work with sinusoidal signal, hence excitation is expressed as :

$$p = \hat{p} e^{i\omega t}$$

$$\ddot{u}_g = a_g = \hat{a}_g e^{i\omega t}$$

where  $\hat{p}$  and  $\hat{a}_g$  are real entities. The real and imaginary parts of  $a_g$  corresponds to a cosine and a sinusoidal input, respectively. The response is taken as :

$$u = \bar{u} e^{i\omega t}$$

$$u_d = \bar{u}_d e^{i\omega t}$$

where  $\bar{u}$  and  $\bar{u}_d$  are complex quantities. Substituting these expressions into the above equations gives [8]:

$$[-m_d \Omega^2 + i c_d \Omega + k_d] \bar{u}_d - m_d \Omega^2 \bar{u} = -m_d \hat{a}_g$$

$$-[i c_d \Omega + k_d] \bar{u}_d + [-m \Omega^2 + k] \bar{u} = -m \hat{a}_g + \hat{p}$$

Solving for  $\bar{u}$  and  $\bar{u}_d$  :

$$\bar{u} = \frac{\hat{p}}{k D_2} [f^2 - \rho^2 + i 2 \xi_d \rho f] - \frac{\hat{a}_g m}{k D_2} [(1 + \bar{m}) f^2 - \rho^2 + i 2 \xi_d \rho f (1 + \bar{m})]$$

$$\bar{u}_d = \frac{\hat{p} \rho^2 - \hat{a}_g m}{k D_2}$$

where:

$$D_2 = [1 - \rho^2][f^2 - \rho^2] - \bar{m} \rho^2 f^2 + i 2 \xi_d \rho f [1 - \rho^2 (1 + \bar{m})]$$

$$f = \frac{\omega_d}{\omega}$$

then converting the solutions to polar solutions :

$$\bar{u} = \frac{\hat{p}}{k} H_1 e^{i\delta_1} - \frac{\hat{a}_g m}{k} H_2 e^{i\delta_2}$$

$$\bar{u}_d = \frac{\hat{p}}{k} H_3 e^{-i\delta_3} - \frac{\hat{a}_g m}{k} H_4 e^{i\delta_4}$$

with :

$$H_1 = \frac{\sqrt{[f^2 - \rho^2]^2 + [2\xi_d \rho f]^2}}{|D_2|}$$

$$H_2 = \frac{\sqrt{[(1 + \bar{m})f^2 - \rho^2]^2 + [2\xi_d \rho f(1 + \bar{m})]^2}}{|D_2|}$$

$$H_3 = \frac{\rho^2}{|D_2|}$$

$$H_4 = \frac{1}{|D_2|}$$

$$|D_2| = \sqrt{([1 - \rho^2][f^2 - \rho^2] - \bar{m}\rho^2 f^2)^2 + (2\xi_d \rho f[1 - \rho^2(1 + \bar{m})])^2}$$

$$\delta_1 = \alpha_1 - \delta_3$$

$$\delta_2 = \alpha_2 - \delta_3$$

$$\tan \delta_3 = \frac{2\xi_d \rho f[1 - \rho^2(1 + \bar{m})]}{[1 - \rho^2][f^2 - \rho^2] - \bar{m}\rho^2 f^2}$$

$$\tan \alpha_1 = \frac{2\xi_d \rho f}{f^2 - \rho^2}$$

$$\tan \alpha_2 = \frac{2\xi_d \rho f(1 + \bar{m})}{(1 + \bar{m})f^2 - \rho^2}$$

In the case where there is no ground acceleration, then  $\hat{a}_g=0$  and  $\bar{u} = \frac{\hat{p}}{k} H_1 e^{i\delta_1}$ . Figure 6 shows the variation of  $H_1$  when  $\bar{m} = 0.05$  (which is a realistic value for a TMD) and  $f = 1$ .

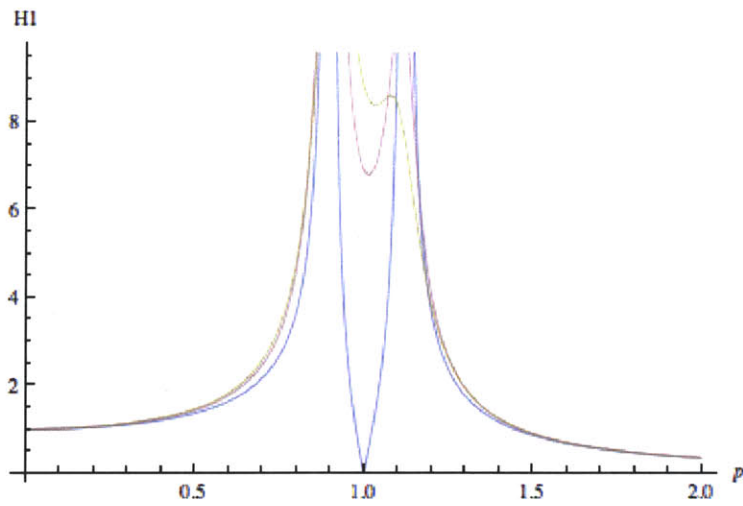


Figure 6: Curve of  $H_1$  as a function of  $\rho$  for  $\xi_d = 0, 0.05$  and  $0.1$  in purple, pink and maroon respectively

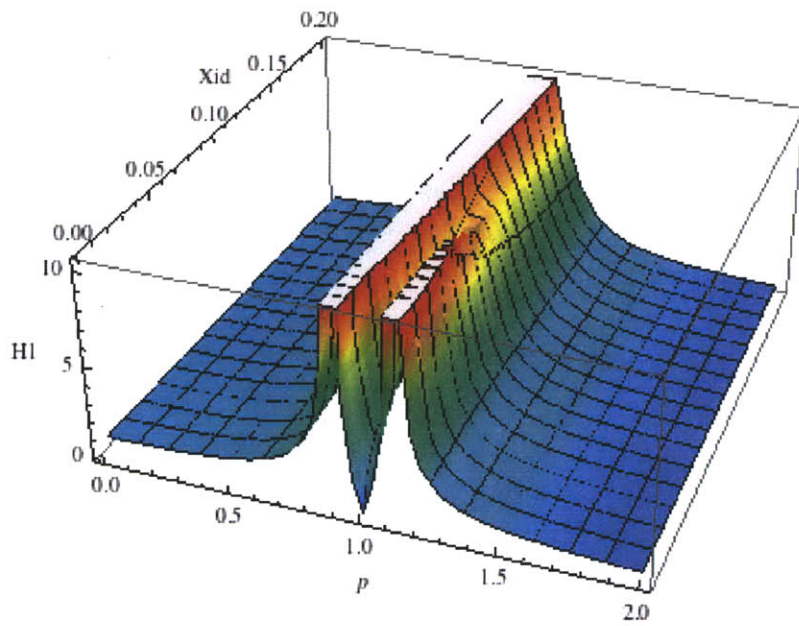


Figure 7: Curve of  $H_1$  as a function of  $\rho$  and  $\xi_d$



Now that the theory of the TMD has been done, let's combine it with piezoelectricity. As explained in the section *Device Concept*, the studied device is a cantilever beam, with piezoelectric material at its base (where the material is the most strained, hence producing more electricity) and a mass on its tip, see Figure 8.

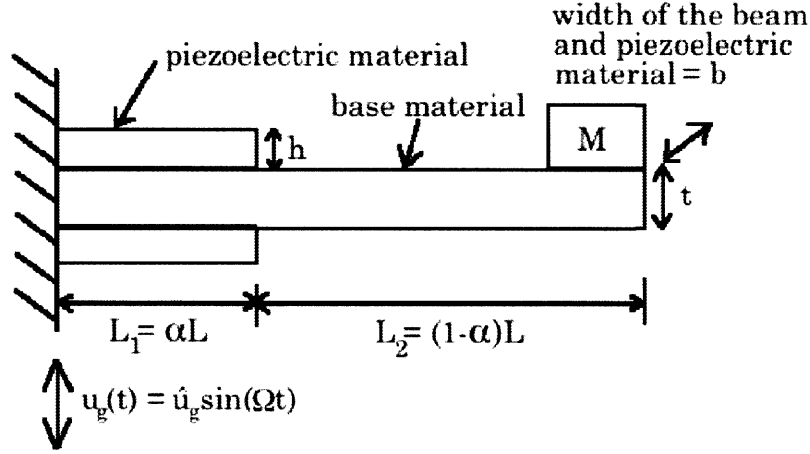


Figure 8: Sketch of the device that is studied

The goal is to study this device behavior when subjected to a harmonic excitation  $p(t) = \hat{p} \sin(\Omega t)$ . The first calculation concerns the stiffnesses of the system, it is obvious that the system will not have the same stiffness along its length :  $L_1$  will be more rigid because of the addition of piezoelectric material. The latter has section property  $(EI)_1$  and  $L_2$  has section property  $(EI)_2$ .  $(EI)_1$  and  $(EI)_2$  both depend on the base material and the piezoelectric material properties. These stiffnesses are given by the following expressions (see Appendix A):

$$k_1 = \frac{6(EI)_1}{[2\alpha^3 + 6(1-\alpha)\alpha^2 + 6(1-\alpha)^2\alpha]L^3}$$

$$k_2 = \frac{3(EI)_2}{(1-\alpha^3)L^3}$$

These expressions make sense because if  $\alpha$  approaches 1, then the whole beam has

a stiffness of  $k_1$  and this quantity approaches  $\frac{3(EI)_1}{L^3}$ , which is in accordance with the beam theory, while  $k_2$  goes to infinity. One can simplify these expressions so that they are only functions of  $E_p$ , the piezoelectric material Young's modulus,  $\gamma$ , the ratio of the Young's modulus of the base material to that of the piezoelectric material, and  $\beta$  the ratio of the thickness of the piezoelectric material  $h$  to that of the base  $t$ . After some calculation, one obtain:

$$k_1 = \frac{6[\gamma + (8\beta^3 + 12\beta^2 + 6\beta)]E_p I}{[2\alpha^3 + 6(1 - \alpha)\alpha^2 + 6(1 - \alpha)^2\alpha]L^3}$$

$$k_2 = \frac{3\gamma E_p I}{(1 - \alpha)^3 L^3}$$

$$I = \frac{bt^3}{12}$$

Now using the theoretical expressions of piezoelectricity (see section *Theory*):

$$\vec{S} = s^E [1 - k_{gen}^2] \vec{T}$$

with :

$$k_{gen}^2 = k^2 \frac{sCZ_{ext}}{1 + sCZ_{ext}}$$

so:

$$\vec{T} = \frac{1}{s^E} \left[ \frac{1 + sCZ_{ext}}{1 + (1 - k^2)sCZ_{ext}} \right] \vec{S}$$

Leading to the expression of  $E_p$ :

$$E_p = \frac{1}{s^E} \left[ \frac{1 + sCZ_{ext}}{1 + (1 - k^2)sCZ_{ext}} \right]$$

The equation of motion for the mass  $M$  can be determined as the system is similar to the one in Figure 9:

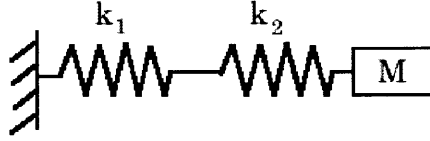


Figure 9: Sketch of the modelisation of the device that is studied

So the two springs in series can be modeled by just one spring of stiffness  $k$  :

$$\frac{1}{k} = \frac{1}{k_1} + \frac{1}{k_2}$$

leading to:

$$k = \frac{AB}{A+B} \frac{E_p I}{L^3}$$

with:

$$A = \frac{6[\gamma + (8\beta^3 + 12\beta^2 + 6\beta)]}{2\alpha^3 + 6(1-\alpha)\alpha^2 + 6(1-\alpha)^2\alpha}$$

$$B = \frac{3\gamma}{(1-\alpha)^3}$$

So the equation of motion is:

$$M\ddot{x} + kx = -M\Omega^2\hat{u}_g\sin(\Omega t)$$

Replacing  $k$  by its expression as well as  $A$ ,  $B$  and  $E_p$ :

$$M\left(1 + \frac{B}{A}\right)\ddot{x} + \frac{BI}{L^3 s E} \left[ \frac{1 + sCZ_{ext}}{1 + (1-k^2)sCZ_{ext}} \right] x = -M\left(1 + \frac{B}{A}\right)\Omega^2\hat{u}_g\sin(\Omega t)$$

One can solve the above equation by assuming  $x = \hat{x}e^{i\Omega t}$  and  $Z_{ext} = R + i\Omega L$ , in accordance with the external circuit shown in Figure 4, and knowing that  $s = i\Omega$  in

the Laplace domain:

$$-\Omega^2 M \left(1 + \frac{B}{A}\right) x + \frac{BI}{L^3 s^E} \left[ \frac{(1 - \Omega^2 LC) + i(\Omega RC)}{1 - (1 - k^2)\Omega^2 CL + i(1 - k^2)\Omega CR} \right] x = -M \left(1 + \frac{B}{A}\right) \Omega^2 \hat{u}_g$$

Finally, one can obtain :

$$\hat{x} = \frac{-M \left(1 + \frac{B}{A}\right)^2 \Omega^2 u_g \sqrt{[f^2 - (1 - k^2)\rho^2]^2 + [(1 - k^2)f^2 \rho \xi_d]^2}}{\sqrt{[f^2 - \rho^2 - (1 + \frac{B}{A})\rho^2(f^2 - \rho^2(1 - k^2))]^2 + [(f^2 \rho \xi_d)(1 - \rho^2(1 - k^2)(1 + \frac{B}{A}))]^2}} e^{i\delta}$$

$$\delta = \alpha_1 - \alpha_2$$

$$\tan \alpha_1 = \frac{f^2 - (1 - k^2)\rho^2}{(1 - k^2)f^2 \rho \xi_d}$$

$$\tan \alpha_2 = \frac{f^2 - \rho^2 - (1 + \frac{B}{A})\rho^2(f^2 - \rho^2(1 - k^2))}{f^2 \rho \xi_d (1 - \rho^2(1 - k^2)(1 + \frac{B}{A}))}$$

also written as :

$$\hat{x} = -M \left(1 + \frac{B}{A}\right)^2 \Omega^2 u_g H_p e^{i\delta}$$

Figure 10 shows different plots of  $H_2$  as a function of  $\rho$  with  $f = 1$ ,  $\frac{B}{A} = 0.2$  and  $k = 0.4$  for different values of  $\xi_d$ .

The similarity between the plots shown in Figure 10 and 11 and the plots for the TMD (Figure 6 and 7) is obvious. The behavior of the piezoelectric generator is very similar to that of a TMD. Like the TMD, there are several points through which all curves pass for the piezoelectric generator, no matter the value of  $\xi_d$ . The tuning of the TMD depends on the mass ratio, while for the piezoelectric material it depends of the ratio  $1 + \frac{B}{A}$ . This similarity between these two systems implies that the method to optimize a piezoelectric system is analogous to the method to tune a TMD. However, it is hard to see the analogy between the two problems when one first look at it. In fact, for the TMD problem, the goal is to minimize the displacement of the main mass while for the piezoelectric material it is to maximize the energy the

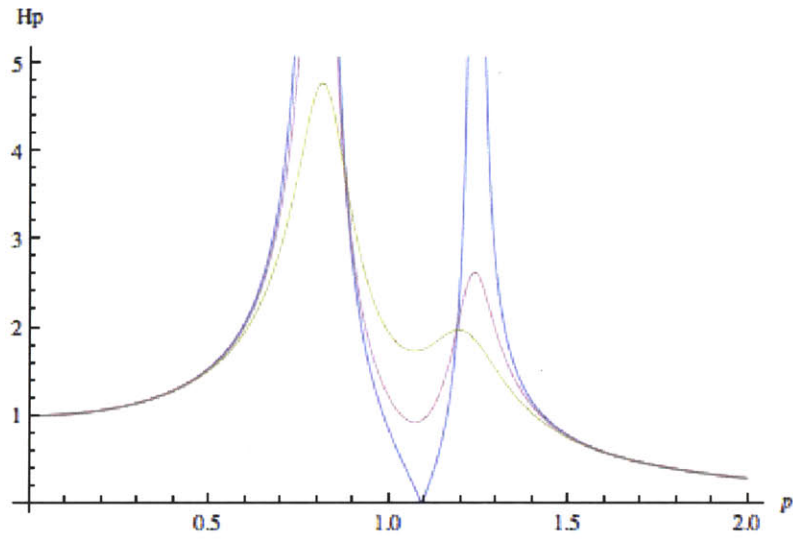


Figure 10: Mathematica file showing a plot of  $H_p$  as a function of  $\rho$  for  $\xi_d=0, 0.2$  and  $0.4$  in purple, pink and maroon respectively

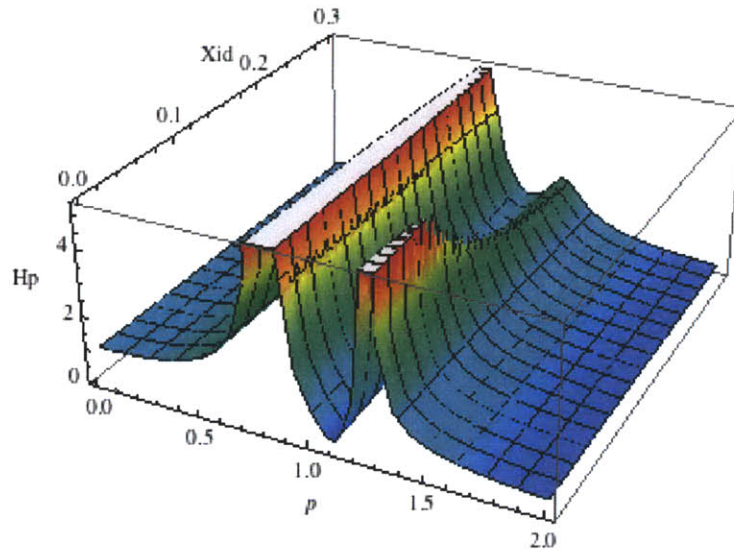


Figure 11: Mathematica file showing a 3D plot of  $H_p$  as a function of  $\xi_d$  and  $\rho$

second system (meaning the shunting circuit) absorbs. But maximizing the secondary system absorption corresponds to maximizing the second's mass displacement, which, for a TMD, would correspond to minimize the main system's motion.

## 6.2 Actuators on Multi-Span Beams

The concept of controlling a structural system to improve its performance and efficiency under varying loading conditions is a relatively new one in the field of structural engineering. Originally proposed by Yao in 1972, structural control takes the approach of viewing structures as complex systems in which performance can be determined by observable measurements and controlling actions can be implemented in order to manipulate that system into behaving desirably (Sangati et al.). There are three primary methods of control: passive, active and semi-active. Each form of structural control has advantages as well as shortcomings and there is large potential for active and semi-active control to truly optimize the behavior of a structural element or system. There is currently much research in the field of control, both on how to exert control forces and to evaluate the state of a structure. The task of controlling a structure, however, becomes more complex when designing for practical applications as the processes of evaluating data in real-time and optimizing communication between elements of the control system are subject to limitations of existing technologies (Lynch). The study of piezoelectric material as actuators is recent and one of the main issue with this kind of material is that they do not develop enough energy for large scale structures. However, they remain very promising as they have a short reaction time. When strained, piezoelectric materials release electricity immediately, and this energy created can be used for the actuators in a very short amount of time.

To better understand the aim of this section, one should be aware of how actuators and controlling systems work. A controlling system is generally made up of three components: the monitoring system, which uses sensors to gather information on a structure, a controller which uses this data to determine the state of a structure, and actuators which respond in accordance with the control system protocol to produce the desired effect on the structure (Sangati et al.) Such a controlling system requires an understanding of the interactions within the structure in order to cre-

ate an algorithm by which the controller can determine the reaction of actuators. These control algorithms may either be static (invariant) as they do not change, or may be adaptive and change over time in order to optimize the control actuation in the structure. Adaptive control systems therefore have a better ability to deal with complex variable or unanticipated loads (Connor 410).

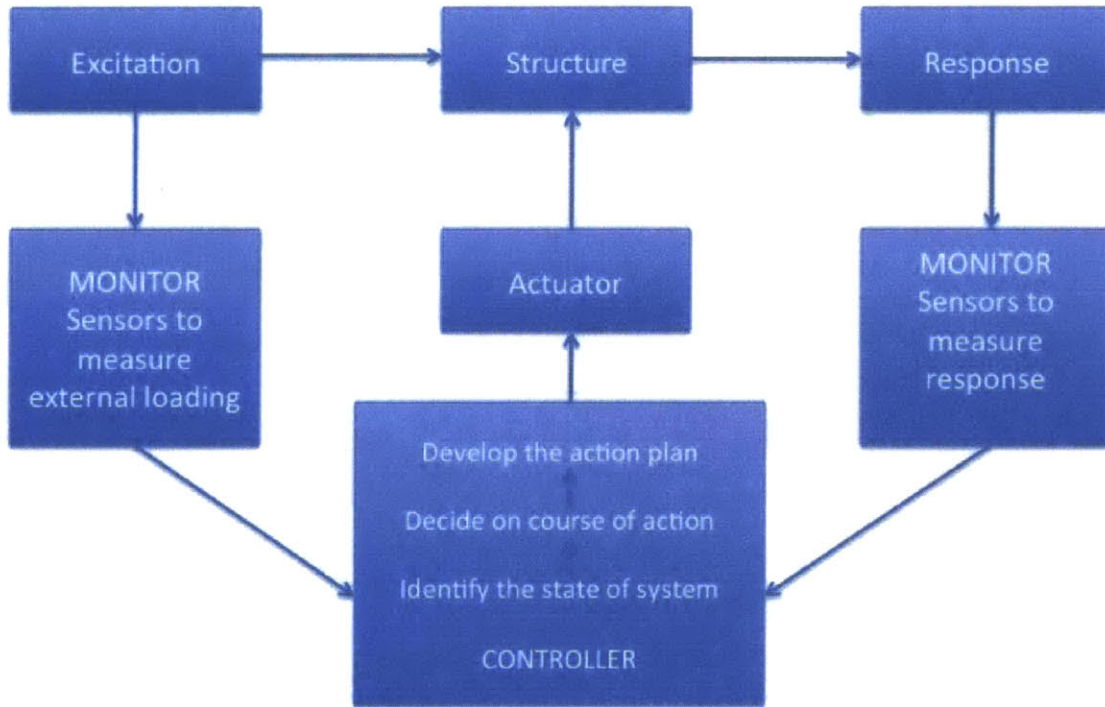


Figure 12: Generic Diagram Representation of a Control Algorithm

Figure 12 shows a generic diagram representation of a control algorithm. The structure experiences some deformations that are represented as the excitation (for example a human being walking on a beam), and sensors record the response of the structure and send the data to controllers that activate (or not) the actuators. The actuators are made to change the structure and thus minimize the bending moment that occurs in its core.



The goal is to use piezoelectric material that would produce electricity with the deformations of the structure and intelligently use this energy to supply the actuators. The main problem is that it is quite complicated to get enough energy with classic piezoelectric materials. They rarely produce the amount of energy required by the actuators for normal structures. So far, most experiments in this area of study have been carried out on a small scale.

The changes in bending moment in a simply supported beam were simulated on Mathematica, for a unit point load running along the beam (see Appendix B for the code). A study of a simply supported beam was performed to understand the concept and make it easier to manipulate, before adding several spans and make the problem indeterminate, and thus more complex and more interesting (see Figure 13).

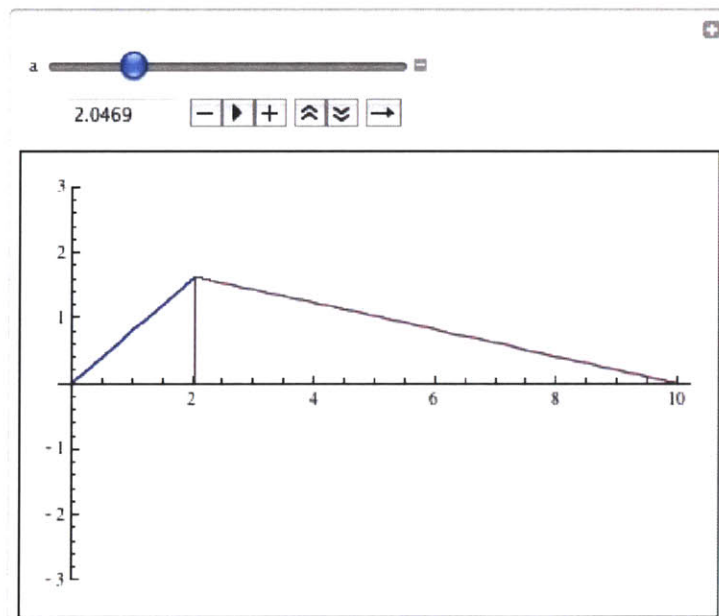


Figure 13: Mathematica file showing the bending moment in a beam with a unit point load running along a beam of length  $L=10$  (it is an animated file, a click on play would animate the feature)

One can see that the maximum moment occurs when the point load is in the middle

of the beam, which is completely logical.

The first problem encountered for the multi-span beam that it is an indeterminate problem. So to be able to make the same animation, moment values were computed from Clapeyron's theorem (theorem of three moments) for an arbitrary position ( $x$ ) of the unit load on the beam. With these values, plotting the changes of bending moments within the beam was not a problem anymore, and the animation was done. Through the animation, it was possible to determine the maximum bending moment for the continuous system; it occurs when the point load is close to the mid-span of the first beam. The maximum value found is:  $M_{max}=6\text{N}\cdot\text{m}$ . The final goal is to lower these moments so that every moment will not exceed the maximum value times a factor  $f$ , this factor under optimal conditions is typically 0.5. So, for this case, every moment has to be lower than  $M_{max} * f$ , yielding a maximum allowable moment of  $3\text{N}\cdot\text{m}$  in absolute value. This is represented by the blue field on the graph: moments should not go over this limit, and stay between these two extreme values.

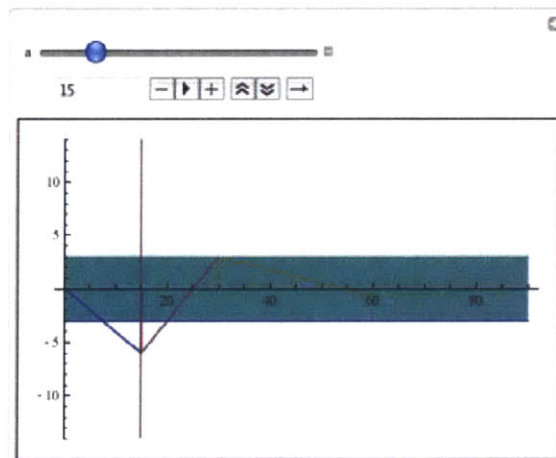


Figure 14: Mathematica file showing the distribution of the bending moments across the beam with the unit point load positioned at 15 ft from the edge of the beam.

Under optimal conditions, the amplitude of the moments of the actuators can be determined, so that the bending moments across the beam do not exceed the critical

moment of 3N-m.

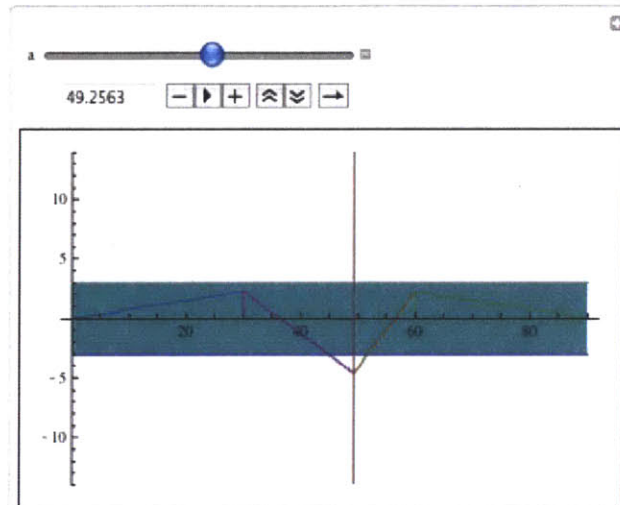


Figure 15: Mathematica file showing the distribution of the bending moments across the beam with the unit point load positioned at 49.25 ft from the edge of the beam.

With the bending diagrams, and the maximum bending moment allowed, the amplitude of the actuators according to time can be figured out. On the Figure 16, one can see the amplitude of the first actuator when the unit point load is situated at  $a=5.15$ .

Then, by adding the bending moments in the beam with those created by the actuators, the final resulting bending moment in the beam can be obtained (see Figure 7).

In the animation, the bending moment stays below the critical moment as predicted, which is the ideal solution. In fact, the bending moment stays right on the limit most of the time, thus saving energy for the actuator which gives only the minimum control force required for the moment to be adequate. One thing that may seem unusual is that the actuator gives its maximum energy when the load is approximately situated at  $a=8.5$  ft (according to the graph) and not at  $a=15$  ft (which is the middle span).

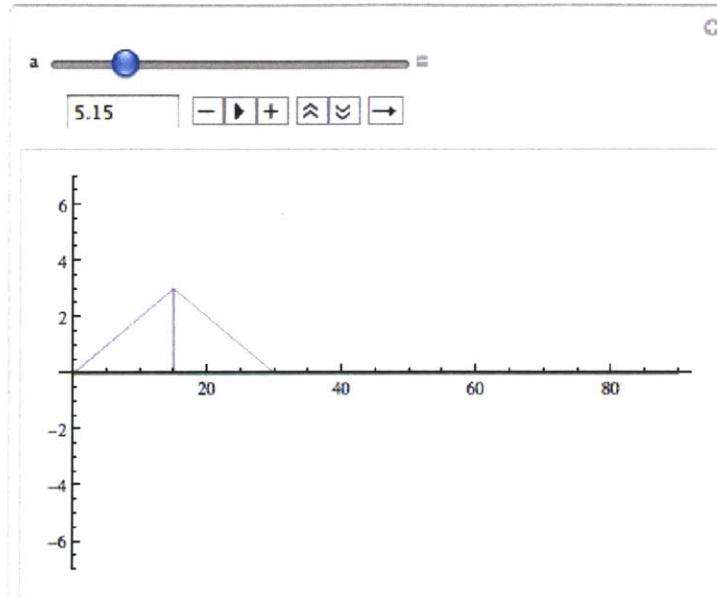


Figure 16: Mathematica file showing amplitude of the actuators when the unit point load is situated at  $a=5.15$  ft

Now knowing the bending moments inside the beam, it is possible to know the stress that occurs on the side of the beam (where the piezoelectric material would be fixed) through the formula :

$$\sigma = \frac{Mz}{I}$$

Thus, with this study one is able to know, for a certain piezoelectric material (meaning a certain  $k$ ) and for a certain multi-span beam, how much energy can be produced through piezoelectricity. This energy would be used to activate actuators whose moments have been figured out and maintain the bending moments below a certain limit fixed beforehand, according to safety factors and regulations (see Figure 17).

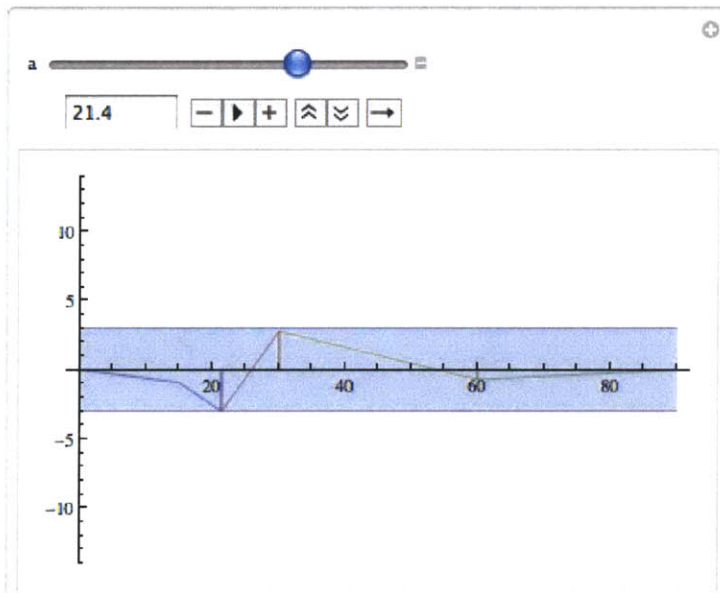


Figure 17: Mathematica file showing the resulting moments after the actuators have been activated

## 7 Conclusion

Piezoelectric materials have many applications in Civil Engineering. Only applications with Tuned-Mass Dampers and Multi-Span Beams have been developed in this thesis. On the one hand, Tuned-Mass Dampers have a behavior very similar to that of an oscillating cantilever beam covered with piezoelectric material and thus the same method used to tune a TMD could also be used to optimize a piezoelectric system. On the other hand the study of Multi-Span Beams have shown that piezoelectric material can be used as actuators to create a moment in the beam, allowing it to support a larger load. Although the magnitudes of piezoelectric voltages, movements, or forces are small, and often require amplification (a typical disc of piezoelectric ceramic will increase or decrease in thickness by only a small fraction of a millimeter, for example) piezoelectric materials have been employed in an impressive range of applications. The piezoelectric effect is used in sensing applications, such as in force or displacement sensors, in transducers to convert electrical energy into vibrational mechanical energy (often sound or ultrasound), in actuators, such as for control of multi-span beams and generators. The limiting issues include the size, weight, and cost of the system. However, since they are compact, simple, and highly reliable, they are a promising solution.

## References

- [1] *Physics Today*, volume 58, 8, p 33, August 2005
- [2] S. Trolier-McKinstry *Chapter3: Crystal Chemistry of Piezoelectric Materials*, 2008.
- [3] E.K. Akdogan *Piezoelectric and Acoustic Materials for Transducer Applications*. New York: Springer.
- [4] *Sensor Sense: Piezoelectric Force Sensors*.
- [5] Chapman and Hall, *Electroceramics: Materials, Properties and Applications.*, New York, NY, 1990.
- [6] <http://www.americanpiezo.com/knowledge-center/piezo-theory/piezoelectricity.html>
- [7] Jerry Czarnecki *A Structural Dynamics Design Methodology for the Optimization of Vibration to Electrical Conversion in Piezoelectric Devices*, Thesis, MIT.
- [8] J. Connor *Introduction to Structural Motion Control*, Massachusetts Institute of Technology, Pearson Education, Inc., 2003.
- [9] *Standard on Piezoelectricity*, ANSI-IEEE 176 (1987).
- [10] <http://www.piezomaterials.com/index.htm>

## A Stiffness Calculations

Here is a sketch of the studied device:

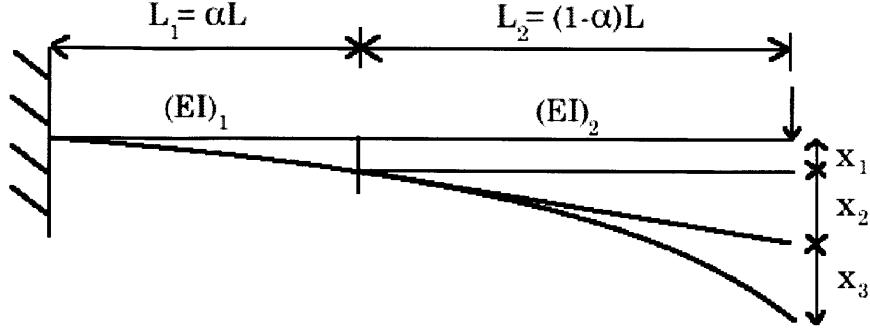


Figure 18: Sketch of the curve of the cantilever for stiffness calculation

The goal is to calculate the stiffnesses of both its parts. The deflection  $x$  can be split into three quantities as shown in Figure 18.

$$x = \left[ \frac{P(\alpha L)^3}{3(EI)_1} + \frac{P(1-\alpha)L(\alpha L)^2}{2(EI)_1} \right] + \left[ (1-\alpha)L \left( \frac{P(\alpha L)^2}{2(EI)_1} + \frac{P(1-\alpha)L(\alpha L)}{(EI)_1} \right) \right] + \left[ \frac{P(1-\alpha)^3 L^3}{(EI)_2} \right]$$

The first two terms represent the deflection due to the load  $P$  and the moment  $P(1-\alpha)L$ , while the last term represents the deflection due to the load and the moment but as if the second member was fixed at the intersection of the two sections. As a result,  $k_1$  and  $k_2$  are:

$$k_1 = \frac{P}{x_1} = \frac{6(EI)_1}{[2\alpha^3 + 6(1-\alpha)\alpha^2 + 6(1-\alpha)^2\alpha]L^3}$$

$$k_2 = \frac{P}{x_2} = \frac{3(EI)_2}{(1-\alpha)^3 L^3}$$



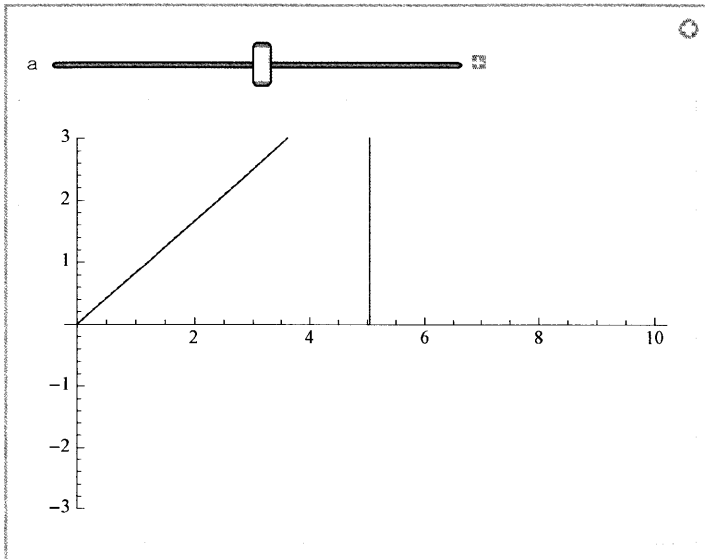
## B Mathematica Code

```

In[78]:= P := 1
L := 10
Manipulate[Plot[{P/L (L - a) x * HeavisideTheta[-x + a], -P/L * a (x - L) * HeavisideTheta[x - a]},
{x, 0, 10}, PlotRange -> 3], {a, 0, 10}]

```

Out[80]=



```

In[84]:= L := 30

```

```

In[85]:= Ma := MB * a / L - (a - a^2 / L)
MB := 4 (a - a^2 / L) (a + L) / (15 L)
MC := - (a - a^2 / L) (a + L) / (15 L)

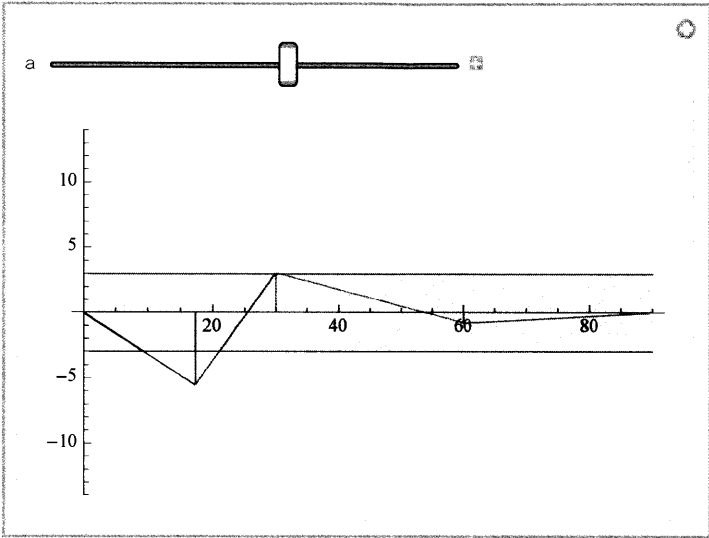
```

```

In[88]:= L := 30
Manipulate[Plot[(((4 (a - a^2 / L) (a + L) / (15 L)) / L - (1 - a / L)) * x * HeavisideTheta[-x + a],
  ((4 (a - a^2 / L) (a + L) / (15 L) - 4 (a - a^2 / L) (a + L) / (15 L) * a / L + (a - a^2 / L)) / (L - a)
  (x - a) + 4 (a - a^2 / L) (a + L) / (15 L) * a / L - (a - a^2 / L)) *
  HeavisideTheta[x - a] * HeavisideTheta[-x + L],
  ((- (a - a^2 / L) (a + L) / (15 L) - 4 (a - a^2 / L) (a + L) / (15 L)) / L (x - L) +
  4 (a - a^2 / L) (a + L) / (15 L)) * HeavisideTheta[x - L] * HeavisideTheta[-x + 2 L],
  (((a - a^2 / L) (a + L) / (15 L)) / L (x - 2 L) - (a - a^2 / L) (a + L) / (15 L)) *
  HeavisideTheta[x - 2 L] * HeavisideTheta[-x + 3 L], 3, -3),
  {x, 0, 3 L}, PlotRange -> 14, Filling -> {5 -> {6}}, {a, 0, L}]

```

Out[89]=



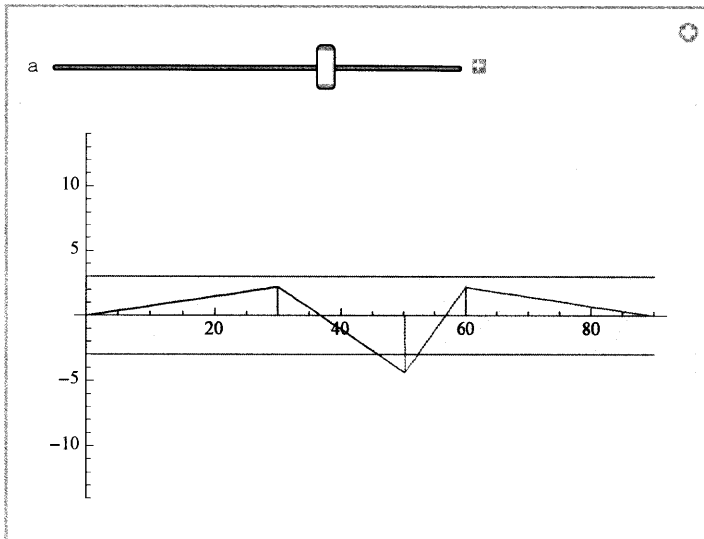
```

In[90]:= L := 30
MB := (a - L - (a - L)^2 / L) a / (5 L)
MC := (a - L - (a - L)^2 / L) a / (5 L)
Ma := (a - L - (a - L)^2 / L) a / (5 L) - (a - L - (a - L)^2 / L)

Manipulate[Plot[{{(a - L - (a - L)^2 / L) a / (5 L) / L x * HeavisideTheta[-x + L],
  (((1 - (a - L) / L) a / (5 L) - (1 - (a - L) / L)) - (1 - (a - L) / L) a / (5 L)) (x - L) +
  (a - L - (a - L)^2 / L) a / (5 L) * HeavisideTheta[x - L] * HeavisideTheta[-x + a],
  (((a - L - (a - L)^2 / L) a / (5 L) - ((a - L - (a - L)^2 / L) a / (5 L) - (a - L - (a - L)^2 / L)) /
  (2 L - a) (x - 2 L) + (a - L - (a - L)^2 / L) a / (5 L)) * HeavisideTheta[x - a] *
  HeavisideTheta[-x + 2 L], (- (a - L - (a - L)^2 / L) a / (5 L) / L (x - 2 L) +
  (a - L - (a - L)^2 / L) a / (5 L)) * HeavisideTheta[x - 2 L], 3, -3},
{x, 0, 3 L}, PlotRange -> 14, Filling -> {5 -> {6}}], {a, L, 2 L}]

```

Out[94]=



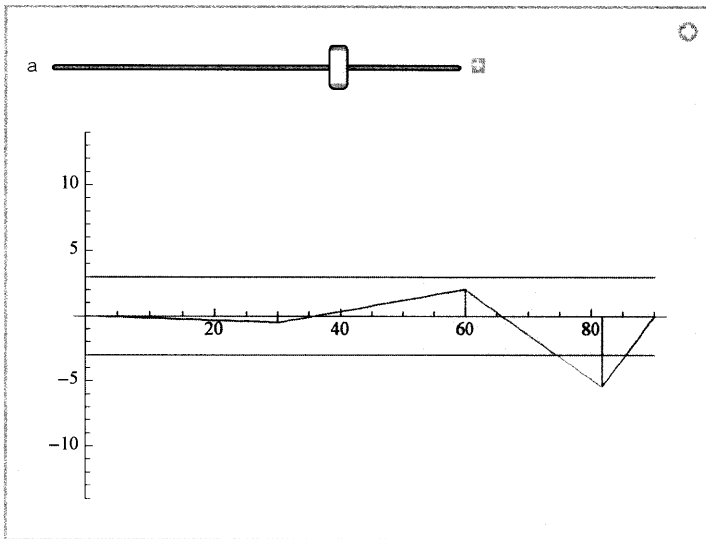
```

In[95]:= L := 30
Ma := 4 (3 L - a - (3 L - a)^2 / L) (3 L - a + L) / (15 L) * (3 L - a) / L - (3 L - a - (3 L - a)^2 / L)
MB := 4 (3 L - a - (3 L - a)^2 / L) (3 L - a + L) / (15 L)
MC := - (3 L - a - (3 L - a)^2 / L) (3 L - a + L) / (15 L)

Manipulate[Plot[{- (3 L - a - (3 L - a)^2 / L) (3 L - a + L) / (15 L) / L x + HeavisideTheta[-x + L],
  ((4 (3 L - a - (3 L - a)^2 / L) (3 L - a + L) / (15 L) + (3 L - a - (3 L - a)^2 / L) (3 L - a + L) / (15 L)) / L
  (x - L) - (3 L - a - (3 L - a)^2 / L) (3 L - a + L) / (15 L)) *
  HeavisideTheta[x - L] * HeavisideTheta[-x + 2 L],
  ((4 (3 L - a - (3 L - a)^2 / L) (3 L - a + L) / (15 L) * (3 L - a) / L - (3 L - a - (3 L - a)^2 / L) -
  4 (3 L - a - (3 L - a)^2 / L) (3 L - a + L) / (15 L)) / (a - 2 L) (x - 2 L) +
  4 (3 L - a - (3 L - a)^2 / L) (3 L - a + L) / (15 L)) * HeavisideTheta[x -
  2 L] * HeavisideTheta[-x + a],
  ((-4 (3 L - a - (3 L - a)^2 / L) (3 L - a + L) / (15 L) * (3 L - a) / L + (3 L - a - (3 L - a)^2 / L)) /
  (3 L - a) (x - 3 L)) * HeavisideTheta[x - a] * HeavisideTheta[-x + 3 L], 3, -3},
{x, 0, 3 L}], PlotRange -> 14, Filling -> {5 -> {6}}, {a, 2 L + 1,
3 L}]

```

Out[99]=

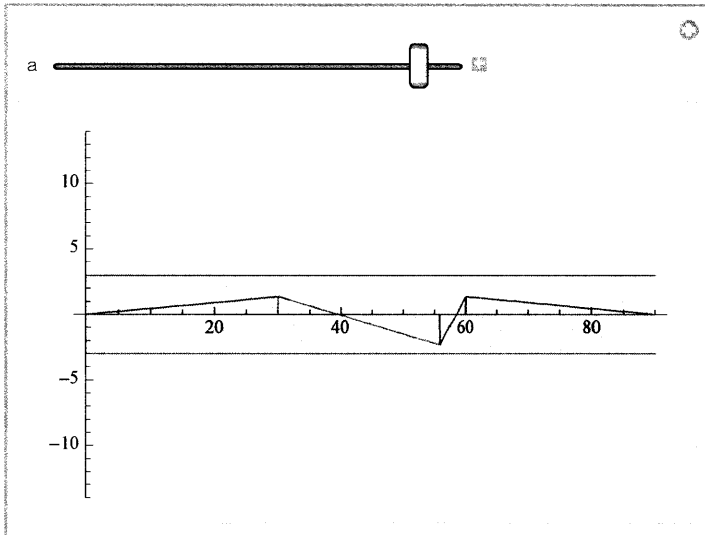


```

In[100]:= Manipulate[
  Plot[{If[a < L, ((4 (a - a^2 / L) (a + L) / (15 L)) / L - (1 - a / L)) * x * HeavisideTheta[-x + a],
    (a - L - (a - L)^2 / L) a / (5 L) / L x * HeavisideTheta[-x + L]], If[a < L,
    ((4 (a - a^2 / L) (a + L) / (15 L) - 4 (a - a^2 / L) (a + L) / (15 L) * a / L + (a - a^2 / L)) / (L - a)
    (x - a) + 4 (a - a^2 / L) (a + L) / (15 L) * a / L - (a - a^2 / L) * HeavisideTheta[x - a] *
    HeavisideTheta[-x + L], (a - L - (a - L)^2 / L) a / (5 L) / L x * HeavisideTheta[-x + L]],
  If[a < L, ((- (a - a^2 / L) (a + L) / (15 L) - 4 (a - a^2 / L) (a + L) / (15 L)) / L (x - L) +
    4 (a - a^2 / L) (a + L) / (15 L)) * HeavisideTheta[x - L] * HeavisideTheta[-x + 2 L],
    (((1 - (a - L) / L) a / (5 L) - (1 - (a - L) / L)) - (1 - (a - L) / L) a / (5 L)) (x - L) +
    (a - L - (a - L)^2 / L) a / (5 L) * HeavisideTheta[x - L] * HeavisideTheta[-x + a]],
  If[a < L, ((- (a - a^2 / L) (a + L) / (15 L) - 4 (a - a^2 / L) (a + L) / (15 L)) / L (x - L) +
    4 (a - a^2 / L) (a + L) / (15 L)) * HeavisideTheta[x - L] * HeavisideTheta[-x + 2 L],
    (((a - L - (a - L)^2 / L) a / (5 L) - ((a - L - (a - L)^2 / L) a / (5 L) - (a - L - (a - L)^2 / L))) /
    (2 L - a) (x - 2 L) + (a - L - (a - L)^2 / L) a / (5 L)) *
    HeavisideTheta[x - a] * HeavisideTheta[-x + 2 L]], If[a < L,
    (((a - a^2 / L) (a + L) / (15 L)) / L (x - 2 L) - (a - a^2 / L) (a + L) / (15 L)) *
    HeavisideTheta[x - 2 L],
    (- (a - L - (a - L)^2 / L) a / (5 L) / L (x - 2 L) + (a - L - (a - L)^2 / L) a / (5 L)) *
    HeavisideTheta[x - 2 L]], 3, -3],
  {x, 0, 3 L}, PlotRange -> 14, Filling -> {6 -> {7}}], {a, 0, 2 L}]

```

Out[100]=

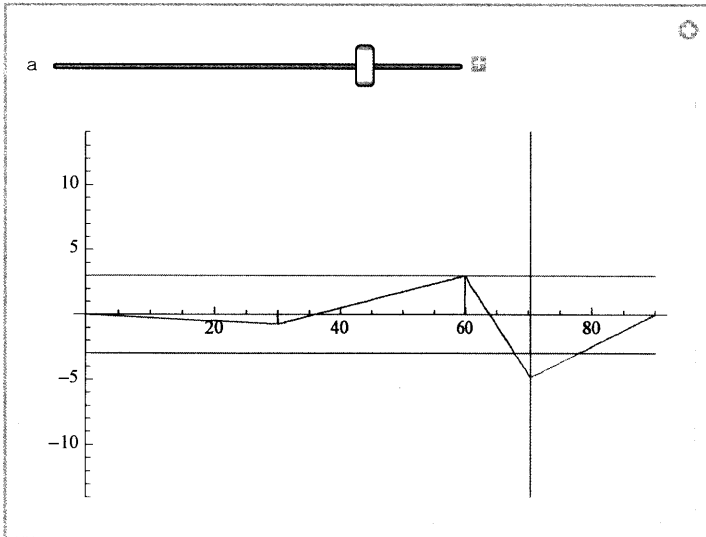


```

In[101]:= Manipulate[
  Plot[{{If[a < L, ((4 (a - a^2 / L) (a + L) / (15 L)) / L - (1 - a / L)) * x * HeavisideTheta[-x + a], 0],
    If[a < L, ((4 (a - a^2 / L) (a + L) / (15 L) - 4 (a - a^2 / L) (a + L) / (15 L) * a / L + (a - a^2 / L) /
      (L - a) (x - a) + 4 (a - a^2 / L) (a + L) / (15 L) * a / L - (a - a^2 / L)) *
      HeavisideTheta[x - a] * HeavisideTheta[-x + L], 0], If[a < L,
      ((- (a - a^2 / L) (a + L) / (15 L) - 4 (a - a^2 / L) (a + L) / (15 L)) / L (x - L) +
      4 (a - a^2 / L) (a + L) / (15 L)) * HeavisideTheta[x - L] * HeavisideTheta[-x + 2 L], 0],
    If[a < L, (((a - a^2 / L) (a + L) / (15 L)) / L (x - 2 L) - (a - a^2 / L) (a + L) / (15 L)) *
      HeavisideTheta[x - 2 L] * HeavisideTheta[-x + 3 L], 0],
    If[L < a < 2 L, (a - L - (a - L)^2 / L) a / (5 L) / L x * HeavisideTheta[-x + L], 0],
    If[L < a < 2 L, (((1 - (a - L) / L) a / (5 L) - (1 - (a - L) / L)) - (1 - (a - L) / L) a / (5 L)) (x - L) +
      (a - L - (a - L)^2 / L) a / (5 L)) *
      HeavisideTheta[x - L] * HeavisideTheta[-x + a], 0], If[L < a < 2 L,
      (((a - L - (a - L)^2 / L) a / (5 L) - ((a - L - (a - L)^2 / L) a / (5 L) - (a - L - (a - L)^2 / L))) /
      (2 L - a) (x - 2 L) + (a - L - (a - L)^2 / L) a / (5 L)) *
      HeavisideTheta[x - a] * HeavisideTheta[-x + 2 L], 0], If[L < a < 2 L,
      (- (a - L - (a - L)^2 / L) a / (5 L) / L (x - 2 L) + (a - L - (a - L)^2 / L) a / (5 L)) *
      HeavisideTheta[x - 2 L], 0], If[a > 2 L,
      - (3 L - a - (3 L - a)^2 / L) (3 L - a + L) / (15 L) / L x * HeavisideTheta[-x + L], 0], If[a > 2 L,
      ((4 (3 L - a - (3 L - a)^2 / L) (3 L - a + L) / (15 L) + (3 L - a - (3 L - a)^2 / L) (3 L - a + L) / (15 L)) /
      L (x - L) - (3 L - a - (3 L - a)^2 / L) (3 L - a + L) / (15 L)) *
      HeavisideTheta[x - L] * HeavisideTheta[-x + 2 L], 0], If[a > 2 L,
      ((4 a^3 - 36 a^2 L + 89 a L^2 - 51 L^3) (2 L - x)
      / (15 L^3) + 4 (3 L - a - (3 L - a)^2 / L) (3 L - a + L) / (15 L)) *
      HeavisideTheta[x - 2 L] * HeavisideTheta[-x + a], 0],
    If[a > 2 L, ((-4 (3 L - a - (3 L - a)^2 / L) (3 L - a + L) / (15 L) / L + (1 - (3 L - a) / L)) (x - 3 L)) *
      HeavisideTheta[x - a] * HeavisideTheta[-x + 3 L], 0], 3, -3, 10 000 (x - a)},
    {x, 0, 3 L}, PlotRange -> 14, Filling -> {13 -> {14}}, {a, 0, 3 L}]

```

Out[101]=

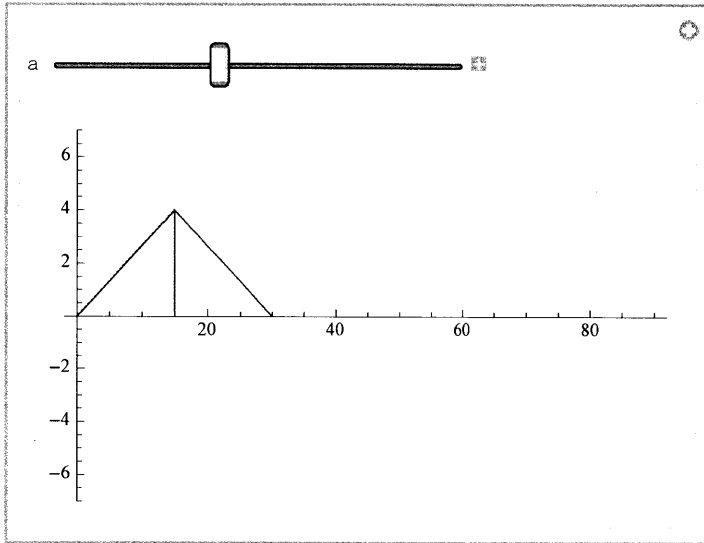


```

In[102]= Manipulate[Plot[{ If[3.5 < a < L/2,
  -((4 (a - a^2 / L) (a + L) / (15 L) / L - (1 - a / L)) a + 3) / a x * HeavisideTheta[-x + L / 2], 0],
  If[3.5 < a < L/2, ((4 (a - a^2 / L) (a + L) / (15 L) / L - (1 - a / L)) a + 3) / a
  (x - L) * HeavisideTheta[x - L / 2] * HeavisideTheta[-x + L], 0],
  If[L/2 < a < L - 6, -((4 (a - a^2 / L) (a + L) / (15 L) / L - (1 - a / L)) a + 3) / (L - a)
  x * HeavisideTheta[-x + L / 2], 0], If[L/2 < a < L - 6,
  ((4 (a - a^2 / L) (a + L) / (15 L) / L - (1 - a / L)) a + 3) / (L - a) (x - L) * HeavisideTheta[x - L / 2] *
  HeavisideTheta[-x + L], 0}], {x, 0, 3 L}, PlotRange -> 7], {a, 0, L}]

```

Out[102]=





```

In[103]:= Manipulate[Plot[(((4 (a - a^2 / L) (a + L) / (15 L)) / L - (1 - a / L)) * x * HeavisideTheta[-x + a] +
  If[3.5 < a <= L / 2, -((4 (a - a^2 / L) (a + L) / (15 L) / L - (1 - a / L)) a + 3) / a x *
    HeavisideTheta[-x + L / 2] * HeavisideTheta[-x + a], 0] + If[L / 2 < a < L - 6,
    -((4 (a - a^2 / L) (a + L) / (15 L) / L - (1 - a / L)) a + 3) / (L - a) x * HeavisideTheta[-x + L / 2],
    0] + If[L / 2 < a < L - 6, ((4 (a - a^2 / L) (a + L) / (15 L) / L - (1 - a / L)) a + 3) / (L - a)
    (x - L) * HeavisideTheta[x - L / 2] * HeavisideTheta[-x + L] * HeavisideTheta[-x + a], 0],
  ((4 (a - a^2 / L) (a + L) / (15 L) - 4 (a - a^2 / L) (a + L) / (15 L) * a / L + (a - a^2 / L) / (L - a)
    (x - a) + 4 (a - a^2 / L) (a + L) / (15 L) * a / L - (a - a^2 / L) *
    HeavisideTheta[x - a] * HeavisideTheta[-x + L] + If[3.5 < a <= L / 2,
    ((4 (a - a^2 / L) (a + L) / (15 L) / L - (1 - a / L)) a + 3) / a
    (x - L) * HeavisideTheta[x - L / 2] * HeavisideTheta[-x + L], 0] +
  If[3.5 < a < L / 2, -((4 (a - a^2 / L) (a + L) / (15 L) / L - (1 - a / L)) a + 3) / a
    x * HeavisideTheta[-x + L / 2] * HeavisideTheta[x - a], 0] +
  If[L / 2 < a < L - 6, ((4 (a - a^2 / L) (a + L) / (15 L) / L - (1 - a / L)) a + 3) / (L - a)
    (x - L) * HeavisideTheta[x - L / 2] * HeavisideTheta[-x + L] * HeavisideTheta[x - a], 0],
  ((- (a - a^2 / L) (a + L) / (15 L) - 4 (a - a^2 / L) (a + L) / (15 L) / L (x - L) +
    4 (a - a^2 / L) (a + L) / (15 L)) * HeavisideTheta[x - L] * HeavisideTheta[-x + 2 L],
  (((a - a^2 / L) (a + L) / (15 L)) / L (x - 2 L) - (a - a^2 / L) (a + L) / (15 L)) *
    HeavisideTheta[x - 2 L] * HeavisideTheta[-x + 3 L], 3, -3),
  {x, 0, 3 L}, PlotRange -> 14, Filling -> {5 -> {6}}, {a, 0, L}]

```

Out[103]=

